Design of pit wall depressurization system – Highland Valley Copper, Logan Lake, BC

Willy Zawadzki[1], Don W. Chorley[1], Al Chance[1], John Scholte[2] & George Warnock[3]
[1] *Golder Associates Ltd., Burnaby, BC, Canada*
[2] *Golder Associates Innovative Applications (GAIA) Inc., Burnaby, BC, Canada*
[3] *Formerly with Highland Valley Copper, Logan Lake, BC, Canada*

ABSTRACT
Highland Valley Copper operates the Valley Pit at a mine in British Columbia. The west wall of the pit is being excavated in a bedrock ridge, while glacial sediments are being exposed in the pit's east wall. In the ultimate pit, silty-clay sediments will be exposed at the base of the overburden slope. The results of stability analyses, together with observed lateral displacements that have occurred to date, indicate that achieving adequate depressurization of these sediments and construction of a toe buttress will be necessary in order to excavate stable ultimate slopes. A pilot depressurization test was conducted in 2004 to evaluate various depressurization methods. Piezometric response recorded during this test was used to develop a numerical hydrogeologic model which was then used to develop a preliminary design of a full-scale depressurization system. This system consisted of approximately 110 vacuum-assisted wells installed near the contact between silty-clay sediments and more permeable overlying strata. The design includes the gradual installation of these wells, as benches become available, between 2005 and 2009, when the northeast wall push-back is scheduled to occur. In 2005 and 2006, 28 vacuum-assisted pumping wells were installed near the pit wall and the pressure response to the pumping of these wells has being monitored in 42 piezometers. Data collected to date indicates that depressurization of the northeast wall is proceeding on schedule.

RÉSUMÉ
Highland Valley Copper exploite la mine à ciel ouvert de Valley Pit en Colombie Britannique. Le substrat rocheux affleure dans la paroi ouest de la mine, et des sédiments glaciaires sont exposés dans la paroi est. Dans la mine définitive, des argiles sableuses seront visibles à la base du mort terrain. Des analyses de stabilité et des observations de déplacements latéraux indiquent que la dépressurisation des sédiments ainsi que la construction d'un contrefort a la base de la pente de mort-terrain seront nécessaires à l'excavation des parois finales stables. Un essai pilote a été mené en 2004 afin d'évaluer diverses méthodes de dépressurisation. La réponse piézométrique enregistrée durant cet essai a été utilisée dans le développement d'un modèle hydrogéologique numérique, lui-même utilisé pour le design préliminaire d'un système de dépressurisation global. Ce système est formé d'environ 110 puits équipés de pompes avec amorçage assisté par le vide, installés près du contact entre les sédiments argilo-silteux et les roches sus-jacentes plus perméables. Ces puits seront installés progressivement au fur et à mesure de l'excavation des bancs entre 2005 et 2009, année prévue pour l'achèvement de la paroi nord-est. En 2005 et 2006, 28 de ces puits ont été installés près de la paroi de la mine et la pression résultant du pompage de ces puits a été mesurée par 42 piézomètres. Les données collectées jusqu'à présent indiquent que la dépressurisation de la paroi nord-est se réalise conformément aux prévisions.

1 INTRODUCTION

Highland Valley Copper operates the Valley, Lornex, and Highmont open pits at the Highland Valley Copper (HVC) mine in south-central British Columbia (Figure 1). The mine, which since 1960's has been producing copper and molybdenum concentrates, is presently the largest base metal mine in Canada. Mining from the low-grade copper porphyry deposit is expected to continue until at least 2019.

Figure 1. Location Plan

The west wall of the Valley Pit is being excavated in a bedrock ridge on the west side of the northwest/southeast trending Highland Valley, while the east wall is being excavated in glacial sediments (Figure 2). Glacial lacustrine silty-clay sediments will be exposed at the base of the overburden slope. The results of stability analyses, together with observed lateral displacements that have occurred to date on the un-daylighted clays behind the existing interim overburden slope, indicate that achieving adequate depressurization in the sediments and construction of a toe buttress will be necessary to excavate stable ultimate overburden slopes.

Figure 2 presents the general stratigraphy of the overburden sediments in the northeast wall of the Valley Pit. In the past, dewatering efforts have focused on the alluvial fan aquifers and the deep Basal Aquifer. The alluvial fan aquifers are generally located above and within the Unit 10A sediments, while the Basal Aquifer is present below the Unit 10C. Substantial dewatering of the Basal Aquifer and the alluvial fan aquifers has occurred since dewatering started in 1986. The water level in the Basal Aquifer is below the bottom of Unit 10C, resulting in gravity drainage from the overlying strata (Unit 10A, 10B, and 10C). Unfortunately, the relatively low permeability of the Unit 10B silty-clays has limited the depressurization achieved in Units 10A and 10B resulting from this drainage.

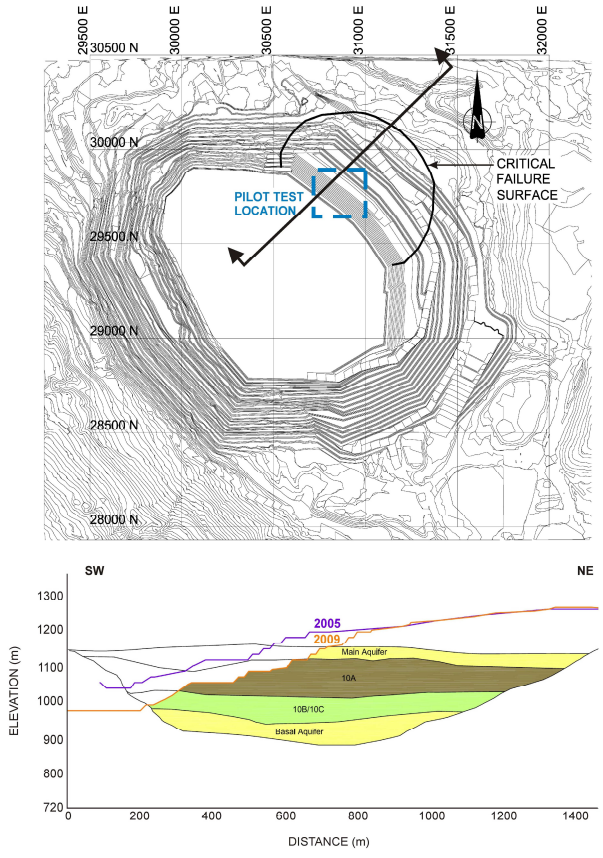

Figure 2. Map Showing the Open Pit and Section with Hydrostratigraphy

2 SLOPE STABILITY CONSIDERATIONS

On the upper northeast wall of the ultimate Valley Pit, approximately 200 meter high slopes will be exposed in glacial overburden sediments. These sediments consist of flat-lying lacustrine sediments overlain by glacio-fluvial sands and gravels and till. The base of the lacustrine sediments contains weak, clay rich, plastic sediments (Unit 10B). Stability investigations have focused on assessing the stability of the overburden slope with respect to deep-seated block sliding along continuous bedding within this clay layer.

The overburden slopes have been gradually exposed in successive pushbacks of the northeast wall of the pit, and the current slope is just over 100 meters high. Until the fall of 2003, the slopes had not exhibited any signs of deep-seated instability, and instability had been limited to bench scale raveling and sloughing of the individual bench faces. Since that time, however, various investigations and observations have confirmed that displacements are occurring within the slope as the result of sliding along the Unit 10B. These observed slope displacements, together with the results of stability analyses carried out in 2004 and 2005, have indicated that it will not be possible to excavate and expose the Unit 10B clays without first depressurizing the lacustrine sediments and installing a substantial buttress at the toe of the slope.

In order to install the buttress, it will be necessary to excavate and expose the Unit 10B clays over a minimum mining width and concurrently install the buttress by backfilling the successive toe excavations. The ability to excavate and maintain the stability of the initial narrow buttress cuts and the proposed buttressed remedial slope configuration will be dependent upon achieving depressurization of the lacustrine sediments of Unit B and the overlying Unit A. Stability analyses have been carried out in 2005 and the location of the critical failure plane with respect to overall stability for the northeast wall is presented in Figure 2. Sufficient depressurization of the Unit 10A and 10B sediments is required for the entire area located within the critical failure surface.

3 SELECTION OF DEPRESSURIZATION METHODS

During the design of the pilot test a number of depressurization methods were considered, including: 1) passive vertical drain wells that would be constructed through Unit 10A and 10B sediments and would be terminated in the underlying and already dewatered Unit 10C; 2) horizontal drainholes drilled along the contact of Units 10A and 10B; 3) conventional vertical wells equipped with submersible pumps and installed into the top of Unit 10B; and 4) vacuum-assisted vertical wells equipped with submersible pumps and installed into the top of Unit 10B.

Methods 1 and 2 were not incorporated in the pilot test program because of concerns that the vertical passive wells could be sheared at the Unit 10A and 10B contact, due to lateral displacement along bedding in the Unit 10B. Such displacement has already been observed within the Unit 10B, and has been observed in other cut

slopes in clay sediments. This could result in the water not being drained down to the dewatered Unit 10C, but draining down and accumulating at the contact between the Unit 10A and 10B, thereby increasing pressures along the failure plane rather than decreasing them. Furthermore, it is difficult to assess the performance of individual passive vertical drain wells as their drainage rates can not be measured directly. This would require the installation of additional observation wells to confirm that sufficient depressurization has occurred. The horizontal drainholes may experience similar problems as the vertical passive drains due to shearing at the contact between Unit 10A and 10B and may be difficult to maintain. Considering all of the above, the passive vertical wells and horizontal drainholes were not included in the pilot test. Thus the pilot test was designed to examine conventional vertical pumping wells and the vacuum-assisted pumping wells.

4 PILOT TEST

The objective of the pilot test was to obtain site-specific hydrogeologic information near the test location so as to provide data for the development of a numerical model for the preliminary design of a full-scale system. The test consisted of installation of six nested piezometers and two vacuum pumping wells (Figure 3), and then short-term and long-term pumping tests in each of the pumping wells. The piezometers were installed at various distances (5 m, 10m, and 15 m) from the pumping wells, with each location equipped with three grouted-in pressure transducer located at various elevations (in Unit 10B, immediately above Unit 10A/10B contact, and in Unit 10A). The placement of these transducers at various distances from the pumping wells and at various elevations resulted in an instrumentation array that allowed the monitoring of the three-dimensional pressure response in Units 10A and 10B resulting from pumping.

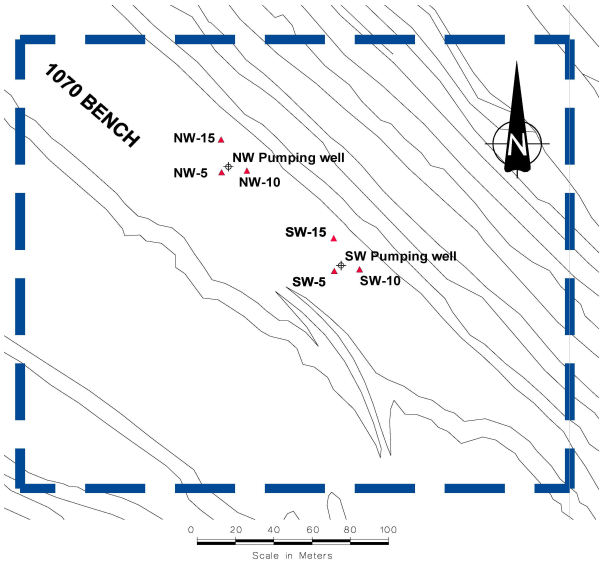

Figure 3. Wells Used during Pilot Test

Short term pumping tests (36 to 48 hour) were conducted in both pumping wells independently, following by a 44-day pumping test. The purpose of these tests were to provide preliminary estimates of the bulk hydraulic conductivity of Units 10A and 10B, assess boundary conditions that will influence the efficiency of the pumping wells, evaluate the long-term performance of the wells, and to provide data to accurately model the depressurization to be achieved in the final full-scale well field. During the 44-day long test both wells were run simultaneously and well discharge rate, air extraction rate, and vacuum in the each well were monitored on hourly basis. The average pumping rate at each well was approximately 22 m^3/day.

Based on the results of the pilot test, it was determined that the vacuum-assisted vertical wells were the optimum depressurization method for the northeast wall. This method provided the maximum water level drawdown, with the vacuum effectively lowering the water level in each well to below the bottom of Unit 10A

The results of the pilot test were analyzed using two methods. First, an analysis was performed using conventional curve-fitting techniques for pumping test analysis that are based on analytical models of well hydraulics. The second method consisted of using a local-scale numerical hydrogeologic model to analyze the pilot test.

4.1 Conventional Curve-fitting Analyses

The response observed during the long-term pilot test was analyzed using AQTESOLV (Duffield, 2007), a commercially available software package for aquifer test analysis. AQTESOLV incorporates several analytical models for the analysis of pumping tests conducted in confined, leaky, and unconfined aquifers. It also allows analyses of variable pumping rates and multiple pumping wells. An example plot showing the drawdown observed during the pilot test in NW-15 (1018 m el.) and best-fit drawdown predicted by the analytical models is presented on Figure 4.

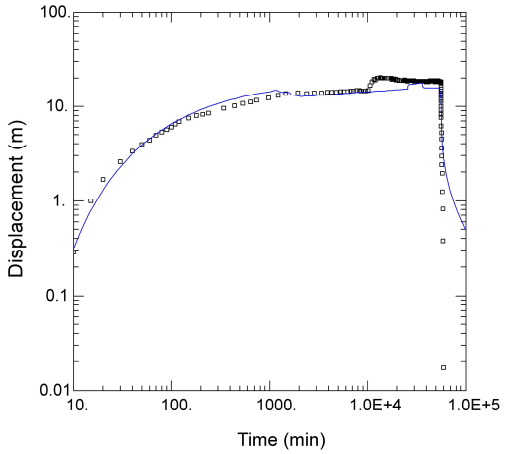

Figure 4. Drawdown Measured during Pilot Test in Piezometer NW-15 at 1018 m el. (squares) and Best-Fit Hantush Solution (line)

The analysis progressed from the least complex analytical model (Theis 1935 solution for a confined aquifer) to more complex models that considered leakage and boundary conditions. Although several analytical models were examined, the analytical solution that provided the best fit to the observed drawdown consisted of the Hantush (1960) leaky aquifer solution with a constant-head boundary located at a distance of approximately 30 m northeast from the pumping wells. This boundary likely represents a water-filled ditch at the foot of the 1085 m bench. In this model, the sandy zone at the base of Unit 10A was assumed to act as a leaky confined aquifer that receives leakage from the overlying less-permeable portion of Unit 10A and from the underlying Unit 10B. The following Table 1 summarizes hydrogeologic parameters that resulted in the best fit to the measured drawdown.

Table 1. Hydrogeologic Parameters from Curve-fitting and Ratio Method

Piezometer	Unit 10A Sandy Zone		Unit 10A		Unit 10B	
	K (m/s)	S_s (1/m)	K (m/s)	S (-)	K (m/s)	S (-)
All	1.2×10^{-6}	2.0×10^{-6}	1.0×10^{-7}	1.0×10^{-4}	1.0×10^{-8}	1.0×10^{-4}
SW-05-1020	1.7×10^{-6}	4.3×10^{-5}	1.0×10^{-7}	1.0×10^{-4}	1.0×10^{-8}	1.0×10^{-4}
SW-10-1024	1.7×10^{-6}	5.2×10^{-5}	1.0×10^{-7}	1.0×10^{-4}	1.0×10^{-8}	1.0×10^{-4}
SW-15-1025	1.3×10^{-6}	5.6×10^{-5}	1.0×10^{-7}	1.0×10^{-4}	1.0×10^{-8}	1.0×10^{-4}
NW-05-1018	1.1×10^{-6}	1.8×10^{-4}	1.0×10^{-7}	1.0×10^{-4}	1.0×10^{-8}	1.0×10^{-4}
NW-10-1023	1.2×10^{-6}	1.2×10^{-4}	1.0×10^{-7}	1.0×10^{-4}	1.0×10^{-8}	1.0×10^{-4}
NW-15-1018	6.2×10^{-7}	1.4×10^{-5}	1.0×10^{-7}	1.0×10^{-4}	1.0×10^{-8}	1.0×10^{-4}

Note: It was assumed that the sandy zone at the base of Unit 10A is 5 m thick.

To assess the vertical hydraulic conductivity of the Unit 10A silts and the Unit 10B silty-clays, the ratio method developed by Neuman and Witherspoon (1972) was employed. In this method, the vertical hydraulic conductivity of these Units is estimated based on assumed values of the specific storage in each Unit, on the measured pressure response, and calculated transmissivity and storativity of the Unit 10A sandy zone. The results of these analyses indicated that the vertical hydraulic conductivity of Unit 10A silts and Unit 10B silty-clays could be 2 to 100 times less than the horizontal hydraulic conductivity of the sandy zone.

4.2 Analysis Based on a Local-Scale Numerical Model

Although the analytical models used in the above analyses incorporate the general features of the flow system near the pilot-test wells, they include several simplifying assumptions that may affect the accuracy of the estimates of hydrogeologic parameters. For example, the analytical model assumes that the constant-head boundary representing the ditch intersects the entire section including the sandy zone at the base of Unit 10A. In reality, this boundary is located at a water-filled ditch at the top of Unit 10A. To address this and other limitations in these methods, additional analysis of the pilot test was undertaken using a local-scale numerical hydrogeologic model. This model was developed using FEFLOW (Diersch, 2007), a finite element modelling code that is capable of simulating transient groundwater flow and transport in three-dimensions under a variety of boundary conditions. Of particular relevance to this analysis is FEFLOW's ability to represent changes in water table elevation in Unit 10A using a deforming mesh.

The model domain (Figure 5) is centered on the pumping wells and extends approximately 500 m northeast from the 1025 m bench. Vertically, the model is divided into 8 layers extending down from the 1070 m elevation bench to the base of Unit 10B at approximately 1000 m elevation. Layers 1 to 5 represent Unit 10A, layer 6 represents the sandy zone at the base of Unit 10A, and layers 7 and 8 represent Unit 10B. Three types of boundary conditions are used in the model. Specified heads are used to represent an inferred seepage face at the 1025 m bench face along the southwest edge of the model and a ditch located at the toe of the 1070 m bench. Specified heads are also applied at the base of the model to simulate leakage from Unit 10B down to the dewatered portion of Unit 10C and the Basal Aquifer and in the sandy portion of Unit 10A along the northeast boundary of the model to represent groundwater inflow from the northeast. A specific flux boundary is applied to the top of the model to simulate recharge from precipitation and downward groundwater flow from portions of the Main Aquifer that are still saturated. All other boundary conditions, which are set at sufficient distance to have negligible influence on the model results, are set to no-flow.

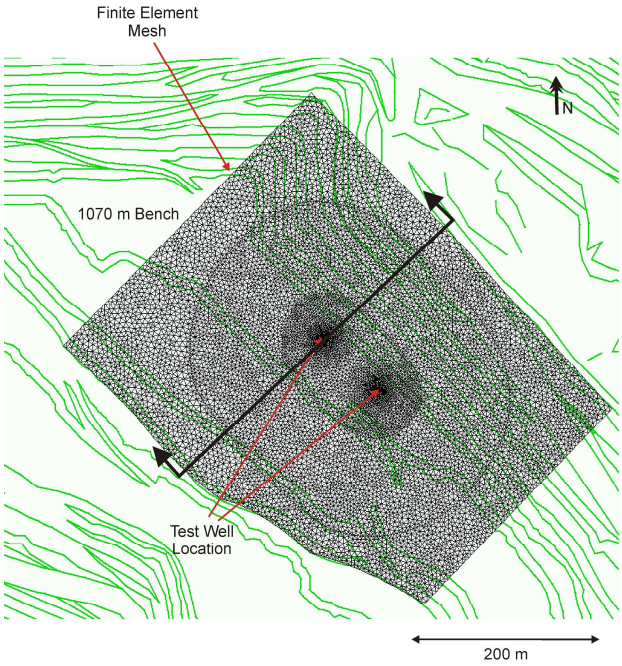

Figure 5. Numerical Model – Pilot Test

Following construction, the model was used to simulate the 44-day pumping test. Pumping rates at the northwest (NW) and southwest (SW) wells were varied in the model based on the values measured during the test. The hydrogeologic parameters determined from curve-

fitting methods were assigned to the finite element mesh. During several calibration trials, these parameters were adjusted until the model-predicted drawdown at the piezometers matched the observed drawdowns reasonably well. Table 2 summarizes model parameters that resulted in the best calibration, whereas Figure 6 show a cross-section with drawdown predicted at the end of the pilot test.

Table 2. Hydrogeologic Parameters from Calibrated Model

Unit	K_h (m/s)	K_h:K_v	S_s (1/m)	S_y (-)
10A	1.0×10^{-7}	5	2.0×10^{-5}	0.25
10A Sandy Zone	2.0×10^{-6}	1	2.0×10^{-5}	0.25
10B	1.0×10^{-8}	2	2.0×10^{-5}	0.25

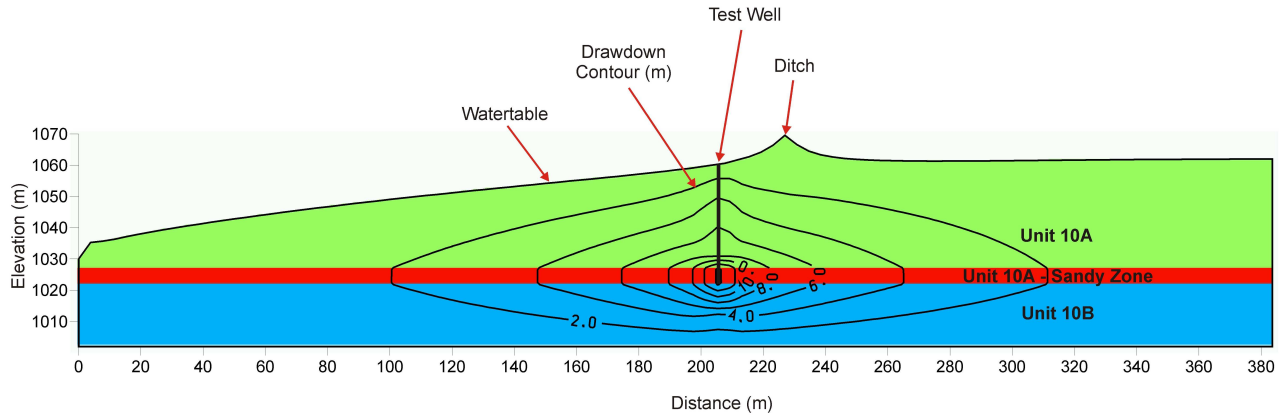

Figure 6. Crossection Showing Drawdown Predicted at the End of the Pumping Test

The hydrogeologic properties of Unit 10A and 10B estimated using the numerical model are in reasonably good agreement with the values derived using the curve-fitting techniques described above. Furthermore, the values determined from the numerical model are considered more accurate as the model was able to better represent the boundary conditions observed at the site and accounted for three-dimensional response to pumping. Thus, these parameters were used in the subsequent design of the full-scale depressurization system.

5 FULL SCALE DEPRESSURIZATION

The results of the pilot test were used to update the conceptual understanding of groundwater conditions near the Valley Pit northeast wall. This understanding was then incorporated into an expanded hydrogeologic model that was then used to design of the full scale depressurization system.

5.1 Conceptual Hydrogeologic Model

A hydrogeological conceptual model is a pictorial and descriptive representation of the groundwater regime that organizes and simplifies the hydrogeology. It must retain enough complexity so that the numerical model developed from it adequately reproduces or simulates the real groundwater flow behaviour. Based on the results of the pilot test and borehole log descriptions, the following describes the conceptual models for the northeast wall under both current conditions and with pumping wells installed.

As shown in Figure 7a, the hydrogeologic regime in the northeast wall of the Valley Pit consists of flat lying and low permeable lacustrine sediments and permeable glacio-fluvial sands and gravels and till. The deepest layer beneath the northeast wall which is pertinent to the present study is Unit 10C which consists of interbedded silts and fine sands that grade coarser downwards. This unit has been found to be virtually dewatered due to downward leakage to the partially dewatered underlying sand and gravel Basal Aquifer. Overlying Unit 10C is Unit 10B which is a low permeable clay-rich lacustrine deposit. The base of this unit experiences some depressurization due to downward leakage to Unit 10C; however, the upper portion of the layer is relatively unaffected by this leakage. Unit 10B is overlain by Unit 10A which consists of sub-horizontal bedded silts and fine sands. Based on the sediment descriptions from boreholes drilled as part of the pilot test and the three-dimensional response in Unit 10A during pumping, the bottom of Unit 10A consists predominantly of fine sand with silt interbeds. This zone is generally more permeable than the overlying predominantly silt portion of Unit 10A. In areas of the pit above an elevation of 1115 m, Unit 10A is overlain by the Main Aquifer, which consists of cross-bedded sands and sandy-gravels. Much of this aquifer has been de-saturated due to ongoing pit dewatering, but deeper portions of this unit are still saturated. As shown in Figure 7a, under present conditions, seepage occurs downwards from the base of Unit 10B to the underlying dewatered Unit 10C and towards the lower bench faces. Unit 10A is recharged in the upper benches by leakage down from saturated portions of the Main Aquifer.

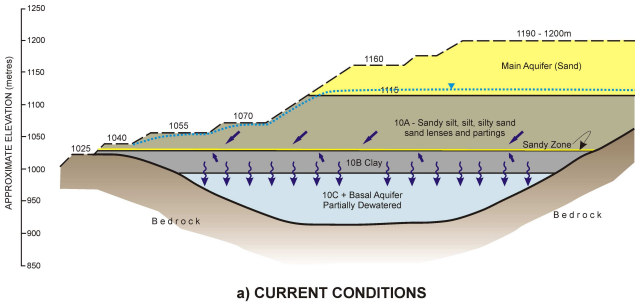

a) CURRENT CONDITIONS

Figure 7a. Conceptual Hydrogeologic Models

As shown in Figure 7b, when the full-scale depressurization system is installed, the sandy zone located at the bottom of Unit 10A will act as an "underdrain", with groundwater from Unit 10A and the upper portion of Unit 10B directed towards this more permeable layer. Necessary depressurization is expected to occur rapidly if a sufficient number of pumping wells are installed, but dewatering Unit 10A is not expected to occur within the mine life. In addition to the depressurization of Unit 10A and 10B, dewatering of the Main Aquifer west of the critical failure plane is required to prevent downward migration of water through vertical cracks that may be caused by slope movement in Unit 10A.

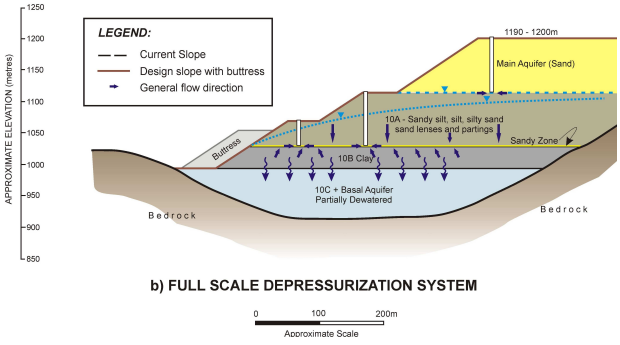

b) FULL SCALE DEPRESSURIZATION SYSTEM

Figure 7b. Conceptual Hydrogeologic Model (white vertical lines represent pumping wells)

5.2 Expanded Numerical Model

The design of the locations and spacings of vacuum-assisted pumping wells in the full scale depressurization system was evaluated using a numerical hydrogeologic model for the entire northeast wall of the Valley Pit. As shown in Figure 8, this model represented an expansion of the numerical model used to analyze the pilot pumping test. The horizontal extent of the model mesh was increased to reflect termination of Unit 10A against bedrock that rises in a northeast from the pit crest. The specified head boundary representing the water filled ditch at the toe of the 1070 m bench was removed under the assumption that water leakage from this ditch would be eliminated through the use of mitigative measures (i.e. low-permeability liners). The specified head boundary assigned along the northeast edge of the pilot test model was removed and a no-flow boundary was assigned further northeast along the edge of the expanded model. This boundary represents the contact between overburden and the lower-permeability bedrock. Other boundary conditions and all hydrogeologic parameters were not modified from the ones used in the pilot test model.

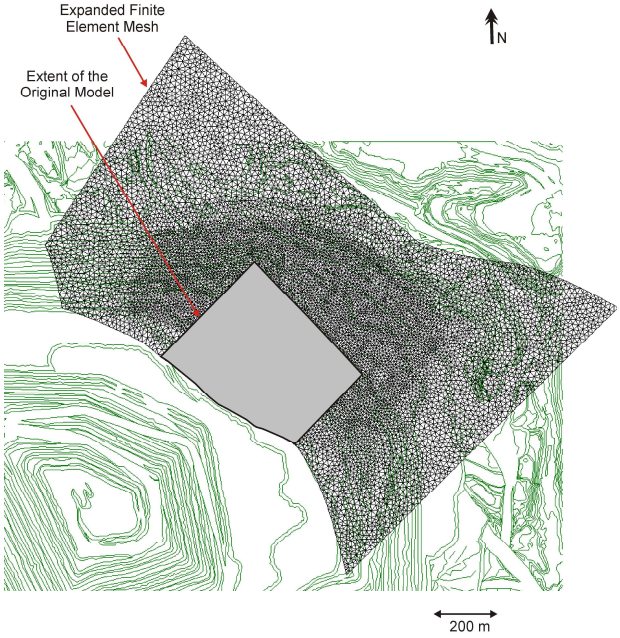

Figure 8. Expanded Numerical Model

5.3 Depressurization System Design

The expanded hydrogeologic model was used to simulate the depressurization system for Units 10A and 10B. Depressurization of Units 10A and 10B are required for the entire 900 m by 500 m area within the critical failure plane as shown on Figure 2. The depressurization must be sufficient during the excavation of the northeast wall to its ultimate configuration and the placement of the buttress. It must also be sufficient for long-term stability once the buttress is in place.

Several simulations trials were conducted to determine the required number and location of pumping wells. During these simulations, the location of the wells and date of their installation was constrained according to the mine plan (i.e. benches on which well can be installed become available at different times). The pumping wells were simulated in the model using a combination of specified head boundaries and discrete feature elements. At the location of each well a specified head boundary was assigned at the base of Unit 10A and was set to 1025 m elevation. In addition, a one-dimensional discrete element was assigned to the nodes along the well casing, from the specified head boundary vertically to the ground surface. The parameters assigned to the discrete element represented the gravel-filled annulus of the pumping well. The approach allowed the simulation of both depressurization resulting from pumping from the well screen and depressurization caused by vertical

drainage towards the well screen through the gravel-filled annulus.

The ultimate configuration of the well field is presented in Figure 9. The depressurization system consists of 110 wells installed in Units 10A and 10B in five rows and pumping at a combined rate of approximately 1,400 m3/day (250 USgpm) and 55 multi-level piezometers. The wells would be installed sequentially between 2005 and 2009. Figure 9 also presents the predicted hydraulic heads at the base of Unit 10A resulting from depressurization in year 2009, whereas Figure 10 presents the predicted pressures in 2009 on a crossection perpendicular to the pit wall. Slope stability analysis indicates that the predicted depressurization provided by these wells is sufficient to maintain stability of the pit walls.

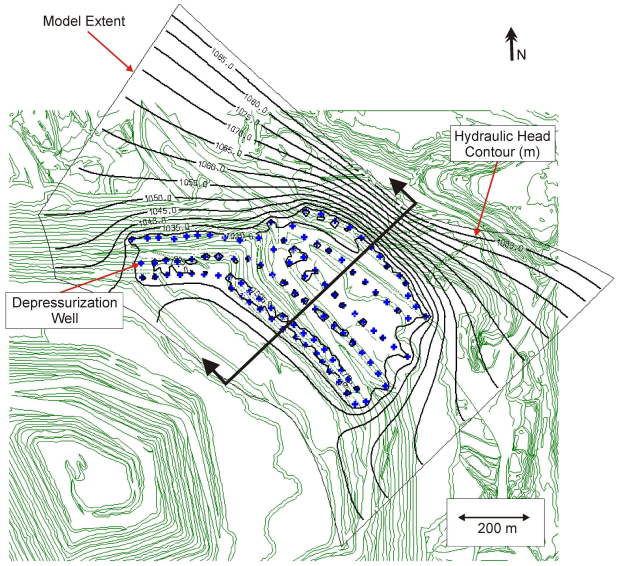

Figure 9. Location of Pumping Wells and Predicted Hydraulic Heads in 2009

6 INSTALLATION PROGRESS

In late 2007, the installation of the pit wall depressurization system was nearly 68% complete, and full system was expected to be in place in early 2009. Monitoring data collected to date from vacuum-assisted pumping wells and 21 multi-level piezometers, together with additional modelling studies, indicate that slope depressurization is proceeding on schedule and that system performance satisfies the design criteria. Based on the observed hydrogeologic response to date and ongoing optimization of the depressurization system, the final number of pumping wells has been decreased from the original estimate of 110 wells to less than 90 wells. Successful depressurization will allow future expansion of the Valley Pit mining to continue at least until year 2019.

REFERENCES

Diersch, H.G. 2007. FEFLOW v. 5.3 Finite Element Subsurface Flow and Transport Simulation System. WASY Institute for Water Resources Planning and System Research Ltd., Berlin, Germany.

Duffield, G.M.., 2007. AQTESOLV for Windows v4.5., User's Guide. HydroSolve Inc., Reston, VA.

Hantush, M.S. 1960. Modification of the theory of leaky aquifers, Jour. of Geophys. Res., 65, no. 11: 3713-3725.

Neuman, S.P., and P.A. Witherspoon. 1972. Field determination of the hydraulic properties of leaky multiple aquifer systems. Water Resources Research 8:1284-1298.

Theis, C.V. 1935. The relation between the lowering of the piezometric surface and rate and duration of discharge of a well using groundwater storage. Trans. Amer. Geophys. Union 2: 519-524.

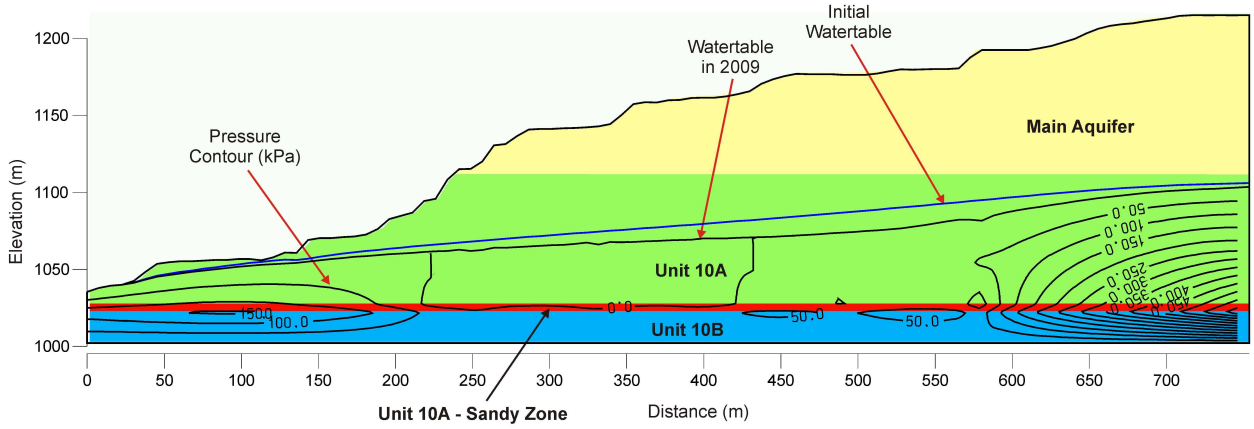

Figure 10. Section Showing Predicted Pressure in 2009